Published in final edited form as:
Mol Cancer Res. 2014 April ; 12(4): 514–526. doi:10.1158/1541-7786.MCR-13-0505.

Inhibition of Focal Adhesion Kinase (FAK) Leads to Abrogation of the Malignant Phenotype in Aggressive Pediatric Renal Malignancies

Michael L. Megison, **Lauren A. Gillory**, **Jerry E. Stewart**, **Hugh C. Nabers**, **Elizabeth Mrozcek-Musulman**, and **Elizabeth A. Beierle**
University of Alabama, Birmingham, Birmingham, AL

Abstract

Despite the tremendous advances in the treatment of childhood kidney tumors, there remain subsets of pediatric renal tumors that continue to pose a therapeutic challenge, mainly malignant rhabdoid kidney tumors and non-osseous renal Ewing sarcoma. Children with advanced, metastatic or relapsed disease have a disease-free survival rate under 30%. Focal adhesion kinase (FAK) is a nonreceptor tyrosine kinase that is important in many facets of tumor development and progression. FAK has been found in other pediatric solid tumors and in adult renal cellular carcinoma, leading us to hypothesize that FAK would be present in pediatric kidney tumors and would impact their cellular survival. In the current study, we showed that FAK was present and phosphorylated in pediatric kidney tumor specimens. We also examined the effects of FAK inhibition upon G401 and SK-NEP-1 cell lines utilizing a number of parallel approaches to block FAK including RNAi and small molecule FAK inhibitors. FAK inhibition resulted in decreased cellular survival, invasion and migration, and increased apoptosis. Further, small molecule inhibition of FAK led to decreased tumor growth in a nude mouse SK-NEP-1 xenograft model. The findings from this study will help to further our understanding of the regulation of tumorigenesis in rare pediatric renal tumors, and may provide desperately needed novel therapeutic strategies and targets for these rare, but difficult to treat, malignancies.

Keywords

FAK; SK-NEP-1 G401; Y15; PF-573,228

Introduction

Significant improvements in the outcome of children with renal malignancies have been achieved over the last 20 years. Advances in medical and surgical care, and the use of cooperative trials have resulted in five year survival rates for Wilms tumor that exceed 90%

Corresponding Author: Elizabeth A. Beierle, MD, 1600 7th Avenue South, ACC Room 300, Birmingham, AL 35233, Phone: (205) 939-9688, Fax: (205) 975-4972, elizabeth.beierle@childrensal.org.

Conflict of Interest: The authors have no conflict of interest or other disclosures.

[1]. There remain, however, subsets of pediatric solid renal tumors that have not recognized a significant improvement in survival. These tumors include malignant rhabdoid kidney tumors and renal Ewing sarcomas. Malignant rhabdoid kidney tumors (MRKT) are aggressive malignancies that comprise 2% of all pediatric renal tumors [2]. Children diagnosed with these tumors often have metastatic disease [2, 3] and despite aggressive treatment, their overall survival rate is less than 30% [2]. Solid organ sarcomas such as extra-osseous renal Ewing sarcomas are also rare and difficult pediatric kidney tumors [4] with a 5-year disease free survival rate less than 50% [5].

Focal adhesion kinase (FAK) is a non-receptor tyrosine kinase that localizes to focal adhesions and controls a number of cellular pathways involved in cell adhesion, migration, invasion, proliferation, and survival [6–9]. FAK activation occurs when cell surface integrins bind to β subunits of FAK, resulting in phosphorylation and binding of Src family kinases [6]. FAK also has an autophosphorylation site at the tyrosine 397 (Y397) residue [10] which leads to increased cell survival via inhibition of detachment-activated apoptosis, or anoikis [11]. FAK is overexpressed in many human adult tumors, including breast and colon cancer [12] as well as the pediatric tumor, neuroblastoma [13]. FAK inhibition with small interfering RNA (siRNA) [14, 15] has been shown to decrease tumor cell survival. However, it is believed that Y397 autophosphorylation site the primary site responsible for the role of FAK in tumor cell migration, invasion and survival. Abrogation of FAK phosphorylation at this site using dominant negative constructs [16] and small molecule inhibitors [15, 17–19], has been shown to decreased tumor cellular migration, invasion, and survival.

In the current study, we hypothesized that rare pediatric renal tumors would express FAK, and that inhibition of FAK would result in a less aggressive phenotype in these cell lines. We demonstrated that abrogation of FAK in renal tumor cell lines resulted in decreased tumor cell survival *in vitro* and decreased xenograft growth *in vivo*. From these studies, we concluded that targeting FAK may prove to be a useful therapeutic modality in the treatment of these rare, but aggressive, pediatric renal tumors.

Methods

Cells and Cell Culture

The renal tumor cell lines G401 and SK-NEP-1 were utilized. The malignant rhabdoid kidney tumor cell line, G401 [20], (CRL-1441, American Type Culture Collection, ATCC, Manassas, VA) was maintained in McCoy's medium (30-2007, ATCC) containing 10% non-heat-inactivated fetal bovine serum (Hyclone, Suwanee, GA), 1 μg/mL penicillin (Gibco, Carlsbad, CA), 1 μg/mL streptomycin (Gibco), and 2 mM L-glutamine (Thermo Fisher Scientific Inc., Waltham, MA) at 37 °C and 5% CO_2. SK-NEP-1 cells, previously described as a renal Ewing's sarcoma [21], were obtained from ATCC (HTB-48,) and maintained in McCoy's medium (ATCC) containing 15% fetal bovine serum (Hyclone), 1 μg/mL penicillin/streptomycin and 2 mM L-glutamine (Thermo Fisher Scientific) at 37 °C and 5% CO_2. Mouse endothelial fibroblasts with ($MEF^{FAK+/+}$) and without ($MEF^{FAK-/-}$) FAK expression provided a control for FAK detection and were a kind gift from Dr. Elena Kurenova [22]. They were maintained under standard conditions in Dulbecco's Modified

Eagle's Medium with 10% fetal bovine serum, 2 mM L-glutamine and 1 μg/mL penicillin/streptomycin.

Antibodies and Reagents

Monoclonal mouse anti-FAK (4.47, 05-0537) and anti-phospho Src (Tyr 416, 05-677) antibodies were obtained from Millipore (EMD Millipore, Billerica, MA) and rabbit polyclonal anti-phospho-FAK (Y397, 71-7900) and anti-phospho Erk 1/2 (05-797R) antibodies were from Invitrogen (Invitrogen Corp., Carlsbad, CA). Rabbit polyclonal anti-PARP (9542S), anti-Akt (9272), anti-phospho Akt (Ser 473, 9271), anti-Erk 1/2 (9102) and anti-cleaved caspase 3 (9662) antibodies were obtained from Cell Signaling Technology (Danvers, MA). Monoclonal mouse anti-Jnk (F-3, sc-1648), anti-phospho Jnk (G-7, sc-6254) and rabbit polyclonal anti-c-Src (sc-18) were from Santa Cruz Biotechnology (Santa Cruz, CA). Monoclonal mouse anti-GAPDH was from Millipore (MAB374) and anti-β-actin was from Sigma (A1978, Sigma-Aldrich Corp., St. Louis, MO). The small molecule PF-573,228 ($C_{22}H_{20}F_3N_5O_3S$) was obtained from Pfizer (New York, NY), and the small molecule 1,2,4,5-benzenetetraamine tetrahydrochloride (Y15) ($C_6H_{10}N_4 \cdot 4ClH$) from Sigma.

Human Tissue Specimens

Formalin-fixed, paraffin-embedded pediatric renal tumor specimens were obtained under waiver of informed consent from the tumor repository at our institution and from the Children's Oncology Group after institutional review board approval (X111123007).

Immunohistochemistry

Formalin-fixed paraffin-embedded human tumor or xenograft tumor specimens were sectioned into 6 μM sections and baked at 70°C for one hour on positive slides. Slides were deparaffinized, steamed, sections quenched with 3% hydrogen peroxide and blocked with BPS blocking buffer (BSA, powdered milk, Triton X-100, PBS) for 30 minutes at 4°C. The primary antibodies anti-FAK (4.47), 1:100 (05-537, Millipore) and anti-phospho-FAK (Y397), 1:100 (04-974, Millipore) were added and incubated overnight at 4°C. After washing with PBS, the secondary antibodies for mouse (ImmPress MP-7402, Vector Laboratories, Burlingame, CA) and rabbit (Super Picture HRP, 87-9263, Zymed Laboratories, Invitrogen) were added 1:250 dilution for 1 hour at 22 °C. The staining reaction was developed with VECTASTAIN Elite ABC kit (PK-6100, Vector Laboratories), TSA™ (biotin tyramide reagent, 1:400, PerkinElmer, Inc., Waltham, MA) and DAB (Metal Enhanced DAB Substrate, Thermo Fisher Scientific). Slides were counterstained with hematoxylin. Negative controls [mouse IgG (1 μg/mL, Invitrogen) or rabbit IgG (1 μg/mL, EMD Millipore)] were included with each run.

Immunohistochemical Scoring

Stained slides of human tumors were reviewed and scored by a pediatric pathologist (E.M.M.) blinded to the patients. The staining was evaluated using a weighted stain score, that graded staining intensity (0, none; 1, weak; 2, moderate; 3, strong) and multiplied it by the percentage of tumor cells within each category. For example, if the specimen showed moderate staining (2) in 40% of the cells, the stain score would be 80 ($2 \times 40 = 80$).

Immunoblotting

Western blots were performed as previously described [19]. Briefly, whole cell lysates or homogenized xenograft specimens were isolated using RIPA [10 mM Tris base pH 7.2, 150 mM NaCl, 1% Na-deoxycholate, 1% Triton X-100, 0.1% sodium dodecyl sulfate (SDS)] or mTOR lysis buffers supplemented with protease inhibitors (Sigma), phosphatase inhibitors (Sigma) and phenylmethanesulfonylfluoride. Lysates were cleared by centrifugation at 14,000 rpm for 30 min at 4 °C. Protein concentrations were determined using BCA Protein Assay Reagent (Pierce, Rockford, IL) and separated by electrophoresis on sodium dodecyl sulfate polyacrylamide (SDS-PAGE) gels. Antibodies were used according to manufacturer's recommended conditions. Molecular weight markers (Precision Plus Protein Kaleidoscope Standards, Bio-Rad, Hercules, CA) confirmed the expected size of the target proteins. Immunoblots were developed with Luminata Classico or Crescendo ECL (EMD Millipore). Blots were stripped with stripping solution (Bio-Rad) at 37 °C for 15 minutes and then reprobed with selected antibodies. Equal protein loading was confirmed with immunoblotting with antibody to GAPDH or β-actin.

siRNA Transfection

Small interfering RNAs (siRNA) were obtained from Qiagen (Qiagen Inc., Valencia, CA) for the following FAK target sequence: 5′-CCGGTCGAATGATAAGGTGTA-3′. Cells were plated (3×10^5 cells per well) and allowed to attach overnight. Cells were treated with HiPerFect® (Qiagen) alone, HiPerFect® plus 20nM Negative Control siRNA (1027310, Qiagen), or HiPerFect® plus FAK siRNA [Hs_PTK2_10 FlexiTube siRNA (NM_005607, Qiagen)] according to manufacturer's protocol, incubated for 24 to 48 hours following transfection and then used for experiments. FAK inhibition by siRNA was confirmed using immunoblotting.

Cell Viability Assays

Cell viability was measured with alamarBlue® assays and trypan blue exclusion. Briefly, 1.5×10^3 cells per well were plated on 96-well culture plates, allowed to attach, and treated with RNAi inhibition, PF-573,228 (PF) (Pfizer), 1,2,4,5-benzenetetraamine tetrahydrochloride (Y15) (Sigma), or both PF and Y15. Following treatment, either 10 μL of alamarBlue® dye (Invitrogen) was added and after 4–6 hours, the absorbance at 595 nm was measured using a kinetic microplate reader (BioTek Gen5, BioTek Instruments, Winooski, VT), or cell viability was determined using trypan blue exclusion and cell counting with a hemacytometer. Viability was reported as fold change.

Migration Assay

Twelve-well culture plates (TransWell®, Corning Inc., Lowell, MA) with 8 μm micropore inserts were used. The bottom side of the insert was coated with collagen Type I (10 mg/mL, 50 μL for 4 hours at 37 °C). G401 cells were treated with PF-573,228 or Y15 and were placed into the upper well at a concentration of 5×10^3 cells per well. Cells were allowed to migrate through the micropore insert for 24 hours. The inserts were then fixed with 3% paraformaldehyde, stained with crystal violet, and migrated cells counted with a light

microscope. Migration was reported as fold change. This assay was only performed with the G401 cells since the SK-NEP-1 cells propagate in a non-adherent fashion.

Cellular Invasion Assay

Similar to migration, twelve-well culture plates (TransWell®, Corning) with 8 μm micropore inserts were used. The top side of the insert was coated with Matrigel™ (BD Biosciences, San Jose, CA) (1 mg/mL, 50 μL for 4 hours at 37 °C). G401 cells were treated with PF-573,228 or Y15 and plated into the upper well at a concentration of 5×10^3 cells per well. Cells were allowed to invade into the Matrigel™ (BD Biosciences) layer for 48 hours. The inserts were then fixed with 3% paraformaldehyde, stained with crystal violet, cells counted with a light microscope and invasion reported as fold change.

Attachment Independent Growth Assay

Attachment independent growth was determined by soft agar assay. A base layer of complete culture media in 1% noble agar was established in 60 mm culture dishes. SK-NEP-1 cells were plated at 1×10^4 cells per dish in the top layer composed of the same culture media and agar mixture. Dishes were treated with graduated concentrations of 1,2,4,5-benzenetetraamine tetrahydrochloride (Y15), and retreated every 4 days. After incubation for 6 weeks, colonies were imaged and quantified using the Gel Dock Imager (Bio-Rad) and Quantity One Software (Bio-Rad), and colony counts reported as fold change.

In Vivo Tumor Growth

Six week old, female, athymic nude mice were utilized (Harlan Laboratories, Inc., Chicago, IL). The mice were maintained in the SPF animal facility with standard 12 hour light/dark cycles and allowed chow and water *ad libitum*. All experiments were performed after obtaining protocol approval by the Institutional Animal Care and Use Committee (120209355) and in compliance with the institutional, national and NIH animal use guidelines. Human renal Ewing sarcoma cells, SK-NEP-1 (1.5×10^6 cells/50 μL sterile PBS) were injected into the subcapsular space of the left kidney. After two weeks, the animals were randomized and began twice daily treatments with intraperitoneal injection of either control vehicle (saline, 100 μL, n=7) or 1,2,4,5-benzenetetraamine tetrahydrochloride (Y15, 15 mg/kg, 100 μL, n=8). Previous experiments with various doses and dosing schedules of the compound proved this dosage to be well tolerated [19, 23]. After two weeks of treatment, the animals were euthanized with CO_2 and bilateral thoracotomy and the kidney tumors and lungs were harvested.

Determination of Metastases

Three levels from each lung of the animals from the SK-NEP-1 xenografts (above) were formalin fixed (10% buffered formalin), paraffin embedded and stained by routine hematoxylin and eosin. Three levels from each lung were examined by a board certified pediatric pathologist (EMM) to determine the presence or absence of metastases.

Data Analysis

Experiments were repeated at least in triplicate, and data reported as mean ± standard error of the mean. Densitometry of western blots was performed using the image histogram analysis feature of Adobe Photoshop® software (Adobe Systems Inc., San Jose, CA). Student's t-test, Fisher's exact test, or ANOVA was used as appropriate to compare data between groups. Statistical significance was determined at the $p<0.05$ level.

Results

Focal adhesion kinase (FAK) was present in pediatric renal tumor specimens and cell lines

Immunohistochemistry was performed on 55 human pediatric renal tumor specimens, including 12 human malignant rhabdoid kidney tumor tissue specimens. Other tumor types included Wilms tumor (19), clear cell sarcoma (12) and mesoblastic nephroma (12). FAK staining was detected in 75% of malignant rhabdoid kidney tumors, compared with 33% of clear cell sarcomas, 32% of Wilms tumors, and 8% of mesoblastic nephromas (Table 1). The number of MRKT specimens staining positive for FAK was significantly greater than those of Wilms tumor or mesoblastic nephroma (Table 1). The median FAK stain score for all tumor types, except the MRKT, was 0 with scores ranging from 0–300 for the Wilms, 0–160 for clear cell sarcoma, and 0–60 for the mesoblastic nephroma tumor specimens. For the MRKT specimens, the median FAK stain score was 15 (range 0–300) (Figure 1B). FAK was phosphorylated in 50% of malignant rhabdoid kidney tumors, compared with 21% of Wilms tumors and 8% of clear cell sarcomas (Table 1). FAK was not phosphorylated in any of the mesoblastic nephroma specimens (Table 1). Representative photomicrographs are presented in Figure 1A. There was weakly positive FAK staining in the normal kidney specimens (no tumor) localized to the renal tubules (Figure 1A, *closed arrows, top left panel*). Staining for phosphorylated FAK was absent in the normal kidney specimens (Figure 1A, *top right panel*). FAK and phospho-FAK staining was also not detected in many Wilms tumor specimens (Figure 1A, *middle panels*). There was strong staining, both for total and phosphorylated FAK, in most of the MRKT specimens (Figure 1A, *brown stain, bottom panels*). Negative controls responded appropriately (Figure 1A, *small box inserts, bottom panels*).

Immunoblotting was used to evaluate FAK expression in the SK-NEP-1 and G401 renal tumor cell lines. SK-NEP-1 and G401 whole cell lysates were compared to those of mouse endothelial fibroblasts with ($MEF^{FAK+/+}$) and without ($MEF^{FAK-/-}$) FAK. FAK was detected in both of the renal tumor cell lines and was phosphorylated (Figure 1C). The FAK expression and phosphorylation in the positive ($MEF^{FAK+/+}$) and negative ($MEF^{FAK-/-}$) cell lysates were appropriate (Figure 1C).

FAK inhibition with small interfering RNA (siRNA) decreased cell survival, migration and invasion

We initially studied the effects of FAK silencing with small-interfering RNA (siRNA) on G401 and SK-NEP-1 cell viability. G401 and SK-NEP-1 cells were treated with HiPerFect® alone (control), HiPerFect® plus negative control siRNA (siNeg), or HiPerFect® plus siRNA specific for FAK (siFAK) for 24 hours. siRNA treatment of the G401 (20 nM) and

the SK-NEP-1 (40 nM) cell lines successfully inhibited FAK protein expression (Figure 2A). FAK was not affected by treatment with HiPerFect® alone (Control) or negative control siRNA (siNeg) (Figure 2A). We also examined the effects of FAK inhibition in the G401 cell line upon upstream and downstream kinases associated with FAK. FAK abrogation with siRNA resulted in decreased phosphorylation of Jnk, Src, and Erk 1/2 (Supplemental Data Figure 1 *C*). Cellular viability was measured using trypan blue exclusion following FAK inhibition with siRNA. In the G401 cells treated with siFAK, cell viability decreased significantly following treatment (1.0 ± 0 vs. 0.65 ± 0.04, $p \leq 0.001$, control vs. siFAK 20nM) (Figure 2B). In the SK-NEP-1 cell line, cell viability also decreased significantly (1.0 ± 0.03 vs. 0.82 ± 0.08, $p \leq 0.001$, control vs. siFAK 40 nM, Figure 2B) following FAK abrogation. Cell viability was not affected by the negative siRNA treatment (Figure 2B). To determine whether cell death was due to apoptosis, cells were treated with siFAK and lysates examined with immunoblotting for PARP cleavage products. In both cell lines, the siFAK-induced cell death was via apoptosis, as demonstrated by increased PARP cleavage products by immunoblotting (Figure 2C). Treatment with negative control siRNA (siNeg) had no affect upon apoptosis in either cell line (Figure 2C).

PF-573,228 inhibited FAK and led to decreased cell survival and motility in G401 and SK-NEP-1 cell lines

To further illustrate the effects of FAK knockdown and prepare for *in vivo* studies, we studied FAK inhibition with a small molecule in both the G401 and SK-NEP-1 cell lines. PF-573,228 (PF) is a small molecule that targets the ATP-binding pocket of FAK and has been shown in multiple cell lines to block FAK phosphorylation at the tyrosine 397 (Y397) site [24]. Cells were treated with PF-573,228 at increasing concentrations. Immunoblotting was utilized to confirm FAK abrogation. After 24 hours of treatment, PF-573,228 decreased FAK phosphorylation in both cell lines (Figure 3A). AlamarBlue® assays were used to assess the effects of PF-induced FAK inhibition on cell survival. Both G401 and SK-NEP-1 cell lines showed significantly decreased cell survival following treatment with PF-573,228 (Figure 3B). The calculated LD_{50} for PF-573,228 in the G401 cell line was 4.7 μM and in the SK-NEP-1 cell line was 11.4 μM. There was an increase in cleaved PARP expression in both cell lines after treatment with PF-573,228 (Figure 3C) indicating that decreased cell viability was due to apoptosis. Caspase 3 cleavage further confirmed apoptosis in the SK-NEP-1 cell line following PF-573,228 treatment (Supplemental Data Figure 1 *A, B*).

FAK also affects cellular migration and invasion [15, 25]; therefore, we wished to determine if these entities would be affected by abrogation of FAK. Due to the non-adherent nature of the cell line, the SK-NEP-1 cells were not amenable to the Transwell® method of studying migration or invasion. G401 cells were treated with increasing concentrations of PF-573,228 and allowed to migrate through the micropore membrane. There was a significant decrease in cellular migration following PF treatment (Figure 3D), and this decrease occurred at concentrations of PF below the calculated LD_{50}. For invasion, G401 cells were treated with increasing concentrations of PF-573,228 and allowed to invade through a Matrigel™ layer. Similar to the migration findings, there was a significant decrease in cellular invasion following PF treatment in the G401 cells (Figure 3E), that again, occurred at concentrations below the calculated LD_{50}.

1,2,4,5-benzenetetraamine tetrahydrochloride (Y15) treatment inhibited FAK and led to decreased cell survival

PF-573,228 was not formulated for use *in vivo* [24] and we wished to advance these studies to an animal model. Therefore, we chose to utilize 1,2,4,5-benzenetetraamine tetrahydrochloride (Y15), one of only a few small molecule FAK inhibitors that can be used in animals [18, 19]. Y15 has been previously described and was designed to inhibit Y397 phosphorylation of FAK [17]. Using immunoblotting, we showed that Y15 treatment resulted in decreased FAK phosphorylation in both the G401 and the SK-NEP-1 cell lines (Figure 4A). Next, we examined how Y15 treatment affected cell survival using alamarBlue® assays. Both G401 and SK-NEP-1 cell lines showed significantly decreased cell survival following treatment with Y15 (Figure 4B). The calculated LD_{50} for Y15 was 3.3 μM in the G401 and 18.2 μM in the SK-NEP-1 cell line. Additionally, the cell death caused by Y15 in both cell lines was via apoptosis, as demonstrated by decreased total PARP and increased PARP cleavage by immunoblotting (Figure 4C, 4D). In the SK-NEP-1 cell line following Y15 treatment there was cleavage of caspase 3 further showing apoptosis (Supplemental Data, Figure 1*B*).

To determine whether the two FAK inhibitors would have synergistic effects when used in combination, we performed alamarBlue® assays with the G401 and SK-NEP-1 cell lines following treatment with PF or Y15 alone and in combination (Supplemental Data, Figure 1 *D*, *E*). The combination index was calculated using the method described by Chou [26] and was nearly one for both cell lines, indicating that these two inhibitors primarily had an additive effect rather than a synergistic effect on cell viability when utilized together (Supplemental Data, Figure 1 *D*, *E*).

FAK inhibition with 1,2,4,5-benzenetetraamine tetrahydrochloride (Y15) decreased cell migration, invasion and attachment independent growth

Phenotypic changes in the G401 and SK-NEP-1 tumor cells following Y15 treatment were further evaluated with cellular migration, invasion, and attachment independent growth assays. G401 cells were treated with increasing concentrations of Y15. After 24 hours the cells showed a marked decrease in migration at concentrations of Y15 below the LD_{50} concentration (Figure 5A). Invasion was also significantly decreased in the G401 cells after Y15 treatment (Figure 5B). Attachment independent growth using soft agar assays is considered one of the best measures of cellular invasion, and was used to measure invasion following Y15-induced FAK inhibition in the SK-NEP-1 cell line. SK-NEP-1 cells were treated with increasing concentrations of Y15, placed into soft agar and colonies were allowed to grow for 6 weeks. The number of cell colonies detected at the end of the studies was decreased by 37.2% at a concentration (10 μM, Y15) compared to controls (Figure 5C); at a concentration below the calculated LD_{50} for Y15 (18.2 μM).

1,2,4,5-benzenetetraamine tetrahydrochloride (Y15) treatment resulted in decreased in vivo tumor growth in a nude mouse model of a pediatric renal tumor

An *in vivo* model of renal tumor growth following FAK inhibition was employed using female athymic nude mice. SK-NEP-1 renal Ewing sarcoma cells (1.5×10^6) were injected into the subcapsular space of the left kidney of each mouse (n = 15). After 2 weeks,

intraperitoneal injections with either control (saline, n = 7) or Y15 (n = 8) at 15 mg/kg bid were initiated. This dose was chosen based upon prior *in vivo* studies with Y15 [17–19, 27]. Y15 treatment continued for 3 weeks, at which time the animals were euthanized and the tumors harvested (Figure 6A). The incidence of tumor occurrence was not different between the treatment groups and all animals (n = 15) developed tumors. Animals treated with Y15 had significantly smaller tumor volumes compared to controls (6198 ± 1500 mm^3 vs. 2706 ± 635 mm^3, control vs. Y15, p = 0.02) (Figure 6B), but Y15 treatment did not affect the weight of the animal (24.8 ± 1.0 g vs. 24.2 ± 1.3 g, control vs. Y15, p = 0.7) nor the weight of the contralateral kidney (0.17 ± 0.02 g vs. 0.21 ± 0.01 g, control vs. Y15, p = 0.09). Immunohistochemistry was performed on formalin-fixed, paraffin-embedded tumor samples for FAK Y397. There was less FAK Y397 staining in the tumors from animals treated with Y15 compared to vehicle treated tumors (Figure 6C). Representative photomicrographs are presented in Figure 6C (40×). Negative controls for both total FAK (mouse IgG) and phospho-FAK (rabbit IgG) reacted appropriately (Figure 6C, *small inserts top panels*). To further confirm target knockdown in the tumor specimens, immunoblotting for FAK was performed on tumor lysates. Tumors treated with Y15 showed a decrease in FAK phosphorylation (Y397) compared to those treated with saline (vehicle). A representative immunoblot is shown in Figure 6D. Densitometry was used to compare immunoblots from a number of xenograft specimens. Phosphorylated FAK was expressed as a ratio to total FAK for each blot and normalized to the β-actin for that blot, allowing for a comparison to be made between the saline treated and the Y15 treated tumors. There was a significant decrease in the FAK phosphorylation (Y397) in the tumors from the animals treated with Y15 (Figure 6E). Since these tumors are known to metastasize to the lungs, we also examined the lung tissue with H & E staining for the presence of metastases. There was no difference in the number of pulmonary metastases in the control versus the treated animals (3.3 ± 0.5 vs. 3.7 ± 0.4 metastases per slide, control vs. Y15, NS).

Discussion

Pediatric renal tumors, other than Wilms tumor, continue to pose a therapeutic challenge, highlighting the need for novel therapies. In this study, we explored the role of FAK in the tumorigenesis of two types of aggressive pediatric renal tumors, malignant rhabdoid kidney tumor and renal Ewing sarcoma. The rationale for the study of FAK in these tumors was three-fold. First, FAK has been shown to play a key role in two other aggressive pediatric solid tumors, neuroblastoma [13, 15] and hepatoblastoma [23]. In neuroblastoma, FAK was important not only for cell survival [13, 28], but also for development of metastases [15]. In hepatoblastoma, FAK inhibition resulted in decreased cell survival *in vitro* and decreased xenograft tumor growth *in vivo* [23]. Second, FAK has been found to be upregulated in the adult renal tumor, renal cell carcinoma (RCC), an aggressive tumor with survival rates around 50%. Jenq and colleagues compared FAK mRNA abundance in a metastatic Caki-1 RCC cell line to that from normal human renal cortex epithelial cells and found that there was a twice as much FAK mRNA in the Caki-1 cell line [29]. Another group examined FAK phosphorylation at the Y861 site by immunohistochemistry in 57 human renal cell carcinoma specimens and noted staining in over 30% of the samples, and on multivariate analysis, there was a correlation between FAK phosphorylation and cancer specific survival

[30]. In another study, decreased FAK activity resulted in decreased renal cell carcinoma cell proliferation and migration [31]. In addition, inhibition of FAK phosphorylation at Y397 in Caki and 786-0 RCC cell lines with the small molecule quinazoline (DZ-50) resulted in decreased viability, reduced adhesion, arrested cell cycle, and reduced metastatic potential *in vivo* [32]. Finally, multiple other kinases that act either upstream or downstream from FAK have been identified as having a significant impact upon the tumorigenicity of other renal cancers. For instance, the upstream kinase, Src has been noted to be overexpressed in metastatic RCC cell lines compared to non-metastatic cell lines [33]. Bai and colleagues tested the Src inhibitor, saracatinib, in Caki-1 and ACHN RCC cell lines and showed decreased cell migration and FAK expression [34]. Akt, a kinase downstream to FAK, has an important role in the progression of RCC. Horiguchi examined 48 RCC specimens for Akt with immunohistochemistry and reported an association between tumor grade and elevated Akt immunostaining [35]. FAK interacts with the Akt pathway to increase tumor cell migration in both breast and colorectal cancers [36, 37]. These previous studies prompted us to hypothesize that FAK would be important in aggressive pediatric renal tumors and supported the need to describe its role in these tumors.

In the current investigations, we reported that FAK was expressed in human pediatric renal tumor specimens, and was more prominent in tumor types that tended to be more aggressive. Our sample numbers were too small to use the FAK stain score as a disease prognosticator, and that was not the purpose of the current study. It was interesting to note, however, that the MRKT had a median stain score of 15 compared to a median score of 0 in the other types of pediatric renal tumors including Wilms tumor. As previously mentioned, MRKTs are highly aggressive tumors with an extremely poor prognosis, compared to Wilms tumors that often have a survival rate greater than 90%. We obtained two different pediatric renal tumor cell lines, G401 (MRKT) and SK-NEP-1 (renal Ewing sarcoma) and confirmed that FAK was present and was phosphorylated at the Y397 site in these cell lines. A review of the literature revealed that the characterization of FAK in pediatric renal tumors and cell lines has not been previously described.

The number of cell lines available for study of these rare, but deadly, pediatric renal tumors is limited. Both the G401 and SK-NEP-1 cell lines were originally thought to be Wilms tumor. The G401 cell line was characterized as a malignant rhabdoid tumor of the kidney, an entity completely distinct from Wilms tumor, by Garvin et al [38]. Subsequently, this cell line has been utilized by numerous investigators to study rhabdoid tumor types. Another cell line that we chose was the SK-NEP-1 cell line. Again, originally classified as a Wilms tumor, this cell line has recently been further characterized and found to express EWS-FL1 gene fusion transcripts, changing the classification of SK-NEP-1 cell line from a Wilms tumor to a non-osseous renal Ewing sarcoma [39]. The SK-NEP-1 cell line was chosen for the current study since non-osseous renal Ewing sarcomas, like MRKT, are rare and clinically difficult to treat tumors.

In the current investigations, it was noted that the SK-NEP-1 cell line had more FAK expression detected by immunoblotting at baseline than the G401 cell line, although the FAK phosphorylation was greater in the G401 cells. These findings may potentially explain the finding that the SK-NEP-1 cell line required a higher concentration of siRNA to

abrogate total FAK expression and increase apoptosis than the G401 cell line. The SK-NEP-1 cells simply had more FAK to knockdown. In addition, the cellular responses to inhibition of FAK phosphorylation with PF-573,228 and Y15 may be explained in a similar fashion. It appeared as if the G401 cell line was more dependent upon FAK phosphorylation for function than the SK-NEP-1 cell line, which may simply be due to the degree of FAK phosphorylation. These findings could also be explained by the idea of oncogene addiction. Investigators have postulated that certain tumor cell lines are physiologically more dependent upon specific survival factors, and inhibition of these specific cellular factors will have a more profound effect upon those cells than others even of the same tumor type [40].

The small molecule FAK inhibitor, PF-573,228 was utilized in these studies to corroborate the siRNA findings that FAK was an important survival signal and a potential target in these rare and difficult to treat renal tumors. PF-573,228 has been shown to block the catalytic activity of FAK by binding to the ATP pocket of FAK [24]. This molecule has been noted to decrease cell survival, migration and invasion in neuroblastoma cell lines [15] as well as decrease metastatic potential of breast cancer cells [41] and enhance chemotherapy-induced cytotoxicity in pancreatic cancer cell lines [42]. Realizing that off-target effects are a risk when using small molecule inhibitors, PF-573,226 was chosen over a similar FAK inhibitor, PF-562,271, in an effort to minimize off-target effects. PF-562,271, in addition to inhibiting FAK, also affects PyK2 [43], which PF-573,228 does not. In this study, PF-573,226 effectively diminished FAK phosphorylation and increased cell death in both the G401 and SK-NEP-1 cell lines. Additionally, this inhibitor also diminished the migration and invasion of the G401 cells at concentrations below the LD_{50} for the cells.

Since we wished to advance our studies to an animal model and PF-573,228 was not suitable for use *in vivo*, another small molecule FAK inhibitor, Y15 (1,2,4,5, benzenetetraamine tetrahydrochloride), was utilized. Again, this small molecule inhibitor was used to corroborate the findings that FAK provided a tumorigenic signal for these tumors. Y15 has been previously described in the literature [17] and has been employed for FAK inhibition *in vitro* [15, 17, 18, 27]. Y15 is also one of only a few small molecule FAK inhibitors available to use in animal studies [17, 19, 27]. In a mouse xenograft model using BT474 human breast cancer cells, animals treated with Y15 (30 mg/kg/day) had significantly smaller tumors than vehicle treated animals [17]. The addition of Y15 to gemcitabine treatment was shown to have an additive affect on survival in a nude mouse model of pancreatic cancer [18]. In another pediatric solid tumor, neuroblastoma, Y15-induced FAK inhibition resulted in a significant decrease in both flank xenograft tumor growth [19] and in liver metastases [27]. These studies provided the rationale for utilizing Y15 as a FAK inhibitor for the current *in vivo* investigation, where we noted that Y15 treatment led to decreased tumor volumes of renal subcapsular SK-NEP-1 tumors.

Pulmonary metastases have been reported with the murine subcapsular renal model of SK-NEP-1 tumors. Although the main focus of the current study was on the importance of FAK in primary tumors and not pulmonary metastases, we did note that Y15 treatment did not alter the prevalence of metastases. This finding may be due to the time lag between the injection of tumor cells and the initiation of treatment. Other investigators have noted similar findings with this model. Soffer and colleagues evaluated the efficacy of topotecan

in reducing tumor growth with SK-NEP-1 cells injected into the subcapsular space of the kidney. They noted a significant decrease in volume of the primary tumor, but no significant change in the occurrence of pulmonary metastases [44]. Lee and others treated mice bearing subcapsular renal SK-NEP-1 xenografts with a selective COX-2 inhibitor, SC-236, and again, demonstrated a profound decrease in the volumes of the primary renal tumors, but no significant effect upon the presence of pulmonary metastases [45].

The small molecules PF-573,228 and Y15 have been reported to inhibit FAK phosphorylation at the Y397 autophosphorylation site [17, 24] and that is why they were chosen for these investigations. Many consider the FAK autophosphorylation site (Y397) to play the primary role in how FAK affects tumor cell migration, invasion and survival. In our study, we did see inhibition of FAK Y397 phosphorylation in both cell lines (Figure 3A and Figure 4A), but at higher concentrations of the inhibitors there was also some inhibition of total FAK expression in both cell lines (Figure 3A and Figure 4A). Other investigators have reported similar findings in other cell lines. Huanwen and colleagues found that pancreatic cancer cells treated with PF-573,228 had a decrease in total FAK expression following treatment with 10 μM concentration [42]. Similar results were noted when colon cancer cells were treated with PF-573,228 [46]. Y15 treatment of the human pancreatic cell line, Panc 1, led to a decrease in FAK phosphorylation but also decreased total FAK at higher concentrations [18]. Findings were similar in BT474 breast cancer cells [17] and U87 glioma cells [47] treated with Y15, in that, increasing concentrations of the inhibitor and also increasing the time of treatment resulted in decreased total FAK expression [17].

In summary, we showed that FAK abrogation, using siRNA and small molecules, had a significant affect upon the malignant phenotype of G401 and SK-NEP-1 cells. There was a significant decrease in cell survival, increased cellular apoptosis and decreased migration and invasion. An important observation was that the changes in migration and invasion following small molecule FAK inhibition occurred at concentrations below the LD_{50} of the inhibitors, since cells that are not viable will not invade or migrate. Another novel aspect of the current studies was the demonstration that FAK inhibition in a nude mouse model incorporating a subcapsular renal tumor resulted in significantly smaller renal tumors when compared to controls. We believe that the data presented provide justification for further investigations of FAK inhibition as a potential therapeutic strategy for difficult to treat pediatric renal tumors.

Supplementary Material

Refer to Web version on PubMed Central for supplementary material.

Acknowledgments

Financial Support: This work was funded in part by grants from the National Cancer Institute including T32CA091078 (M.L.M and L.A.G.) and K08CA118178 (E.A.B.).

The authors would like to thank Dr. Elena Kurenova, Roswell Park Cancer Institute, Buffalo, NY, for her kind gift of the FAK positive ($MEF^{FAK+/+}$) and negative ($MEF^{FAK-/-}$) mouse endothelial fibroblast cell lines.

References

1. Dome JS, Fernandez CV, Mullen EA, Kalapurakal JA, Geller JI, Huff V, et al. COG Renal Tumors Committee. Children's Oncology Group's 2013 blueprint for research: renal tumors. Pediatr Blood Cancer. 2013; 60:994–1000. [PubMed: 23255438]
2. Zhuge Y, Cheung MC, Yang R, Perez EA, Koniaris LG, Sola JE. Pediatric non-Wilms renal tumors: subtypes, survival, and prognostic indicators. J Surg Res. 2010; 163:257–63. [PubMed: 20538287]
3. van den Heuvel-Eibrink MM, van Tinteren H, Rehorst H, Coulombe A, Patte C, de Camargo B, et al. Malignant rhabdoid tumours of the kidney (MRTKs), registered on recent SIOP protocols from 1993 to 2005: a report of the SIOP renal tumour study group. Pediatr Blood Cancer. 2011; 56:733–7. [PubMed: 21370404]
4. Rodriguez-Galindo C, Marina NM, Fletcher BD, Parham DM, Bodner SM, Meyer W, et al. Is primitive neuroectodermal tumor of the kidney a distinct entity? Cancer. 1997; 79:2243–50. [PubMed: 9179073]
5. Kushner BH, Hajdu SI, Gulati SC, Erlandson RA, Exelby PR, Lieberman PH. Extracranial primitive neuroectodermal tumors. The Memorial Sloan-Kettering Cancer Center experience. Cancer. 1991; 67:1825–9. [PubMed: 1848468]
6. Xing Z, Chen HC, Nowlen JK, Taylor SJ, Shalloway D, Guan JL. Direct interaction of v-Src with the focal adhesion kinase mediated by the Src SH2 domain. Mol Biol Cell. 1994; 5:413–21. [PubMed: 8054685]
7. Schaller MD, Borgman CA, Cobb BS, Vines RR, Reynolds AB, Parsons JT. pp125FAK a structurally distinctive protein-tyrosine kinase associated with focal adhesions. Proc Natl Acad Sci U S A. 1992; 89:5192–6. [PubMed: 1594631]
8. Hanks SK, Polte TR. Signaling through focal adhesion kinase. Bio Essays. 1997; 19:137–45.
9. Gabarra-Niecko V, Schaller MD, Dunty JM. FAK regulates biological processes important for the pathogenesis of cancer. Cancer Metastasis Rev. 2003; 22:359–74. [PubMed: 12884911]
10. Chen HC, Guan JL. Association of focal adhesion kinase with its potential substrate phosphatidylinositol 3-kinase. Proc Natl Acad Sci U S A. 1994; 91:10148–52. [PubMed: 7937853]
11. Schlaepfer DD, Hauck CR, Sieg DJ. Signaling through focal adhesion kinase. Prog Biophys Mol Biol. 1999; 71:435–78. [PubMed: 10354709]
12. Cance WG, Harris JE, Iacocca MV, Roche E, Yang X, Chang J, et al. Immunohistochemical analyses of focal adhesion kinase expression in benign and malignant human breast and colon tissues: correlation with preinvasive and invasive phenotypes. Clin Cancer Res. 2000; 6:2417–23. [PubMed: 10873094]
13. Beierle EA, Massoll NA, Hartwich J, Kurenova EV, Golubovskaya VM, Cance W, et al. Focal adhesion kinase expression in human neuroblastoma: immunohistochemical and real-time PCR analyses. Clin Cancer Res. 2008; 14:3299–305. [PubMed: 18519756]
14. Han EK, Mcgonigal T, Wang J, Giranda VL, Luo Y. Functional analysis of focal adhesion kinase (FAK) reduction by small inhibitory RNAs. Anticancer Res. 2004; 24:3899–905. [PubMed: 15736429]
15. Megison ML, Stewart JE, Nabers HC, Gillory LA, Beierle EA. FAK inhibition decreases cell invasion, migration and metastasis in MYCN amplified neuroblastoma. Clin Exp Metastasis. 2012; 30:555–68. [PubMed: 23208732]
16. Beierle EA, Ma X, Trujillo A, Kurenova EV, Cance WG, Golubovskaya VM. Inhibition of focal adhesion kinase and src increases detachment and apoptosis in human neuroblastoma cell lines. Mol Carcinog. 2010; 49:224–34. [PubMed: 19885861]
17. Golubovskaya VM, Nyberg C, Zheng M, Kweh F, Magis A, Ostrov D, et al. A small molecule inhibitor, 1,2,4,5-benzenetetraamine tetrahydrochloride, targeting the y397 site of focal adhesion kinase decreases tumor growth. J Med Chem. 2008; 51:7405–16. [PubMed: 18989950]
18. Hochwald SN, Nyberg C, Zheng M, Zheng D, Wood C, Massoll NA, et al. A novel small molecule inhibitor of FAK decreases growth of human pancreatic cancer. Cell Cycle. 2009; 8:2435–43. [PubMed: 19571674]

19. Beierle EA, Ma X, Stewart J, Nyberg C, Trujillo A, Cance WG, et al. Inhibition of focal adhesion kinase decreases tumor growth in human neuroblastoma. Cell Cycle. 2010; 9:1005–15. [PubMed: 20160475]
20. Smith MA, Morton CL, Phelps D, Girtman K, Neale G, Houghton PJ. SK-NEP-1 and Rh1 are Ewing family tumor lines. Pediatr Blood Cancer. 2008; 50:703–6. [PubMed: 17154184]
21. Garvin AJ, Re GG, Tarnowski BI, Hazen-Martin DJ, Sens DA. The G401 cell line, utilized for studies of chromosomal changes in Wilms' tumor, is derived from a rhabdoid tumor of the kidney. Am J Pathol. 1993; 142:375–80. [PubMed: 8382007]
22. Kurenova E, Xu LH, Yang X, Baldwin AS Jr, Craven RJ, Hanks SK, et al. Focal adhesion kinase suppresses apoptosis by binding to the death domain of receptor-interacting protein. Mol Cell Biol. 2004; 24:4361–71. [PubMed: 15121855]
23. Gillory LA, Stewart JE, Megison ML, Nabers HC, Mroczek-Musulman E, Beierle EA. FAK Inhibition Decreases Hepatoblastoma Survival Both In Vitro and In Vivo. Transl Oncol. 2013; 6:206–15. [PubMed: 23544173]
24. Slack-Davis JK, Martin KH, Tilghman RW, Iwanicki M, Ung EJ, Autry C, et al. Cellular characterization of a novel focal adhesion kinase inhibitor. J Biol Chem. 2007; 282:14845–52. [PubMed: 17395594]
25. Hauck CR, Sieg DJ, Hsia DA, Loftus JC, Gaarde WA, Monia BP, et al. Inhibition of focal adhesion kinase expression or activity disrupts epidermal growth factor-stimulated signaling promoting the migration of invasive human carcinoma cells. Cancer Res. 2001; 61:7079–90. [PubMed: 11585739]
26. Chou TC. Drug combination studies and their synergy quantification using the Chou-Talalay method. Cancer Res. 2010; 70:440–6. [PubMed: 20068163]
27. Lee S, Qiao J, Paul P, O'Connor KL, Evers MB, Chung DH. FAK is a critical regulator of neuroblastoma liver metastasis. Oncotarget. 2012; 3:1576–87. [PubMed: 23211542]
28. Beierle EA, Trujillo A, Nagaram A, Kurenova EV, Finch R, Ma X, et al. N-MYC regulates focal adhesion kinase expression in human neuroblastoma. J Biol Chem. 2007; 282:12503–16. [PubMed: 17327229]
29. Jenq W, Cooper DR, Ramirez G. Integrin expression on cell adhesion function and up-regulation of P125FAK and paxillin in metastatic renal carcinoma cells. Connect Tissue Res. 1996; 34:161–74. [PubMed: 9023046]
30. Qayyum T, McArdle PA, Lamb GW, Jordan F, Orange C, Seywright M, et al. Expression and prognostic significance of Src family members in renal clear cell carcinoma. Br J Cancer. 2012; 107:856–63. [PubMed: 22814579]
31. Brenner W, Greber I, Gudejko-Thiel J, Beitz S, Schneider E, Walenta S, et al. Migration of renal carcinoma cells is dependent on protein kinase Cdelta via beta1 integrin and focal adhesion kinase. Int J Oncol. 2008; 32:1125–31. [PubMed: 18425341]
32. Sakamoto S, Schwarze S, Kyprianou N. Anoikis disruption of focal adhesion-Akt signaling impairs renal cell carcinoma. Eur Urol. 2011; 59:734–44. [PubMed: 21269758]
33. Yonezawa Y, Nagashima Y, Sato H, Virgona N, Fukumoto K, Shirai S, et al. Contribution of the Src family of kinases to the appearance of malignant phenotypes in renal cancer cells. Mol Carcinog. 2005; 43:188–97. [PubMed: 15864803]
34. Bai L, Yang JC, Ok JH, Mack PC, Kung HJ, Evans CP. Simultaneous targeting of Src kinase and receptor tyrosine kinase results in synergistic inhibition of renal cell carcinoma proliferation and migration. Int J Cancer. 2012; 130:2693–702. [PubMed: 21792888]
35. Horiguchi A, Oya M, Uchida A, Marumo K, Murai M. Elevated Akt activation and its impact on clinicopathological features of renal cell carcinoma. J Urol. 2003; 169:710–3. [PubMed: 12544348]
36. Schnater JM, Bruder E, Bertschin S, Woodtli T, de Theije C, Pietsch T, et al. Subcutaneous and intrahepatic growth of human hepatoblastoma in immunodeficient mice. J Hepatol. 2006; 45:377–86. [PubMed: 16780998]
37. Turecková J, Vojtechová M, Krausová M, Sloncová E, Korínek V. Focal adhesion kinase functions as an akt downstream target in migration of colorectal cancer cells. Transl Oncol. 2009; 2:281–90. [PubMed: 19956390]

38. Garvin AJ, Re GG, Tarnowski BI, Hazen-Martin DJ, Sens DA. The G401 cell line, utilized for studies of chromosomal changes in Wilms' tumor, is derived from a rhabdoid tumor of the kidney. Am J Pathol. 1993; 142:375–80. [PubMed: 8382007]
39. Smith MA, Morton CL, Phelps D, Girtman K, Neale G, Houghton PJ. SK-NEP-1 and Rh1 are Ewing family tumor lines. Pediatr Blood Cancer. 2008; 50:703–6. [PubMed: 17154184]
40. Weinstein IB. Cancer. Addiction to oncogenes – the Achilles heal of cancer. Science. 2002; 297:63–4. [PubMed: 12098689]
41. Wendt MK, Schiemann WP. Therapeutic targeting of the focal adhesion complex prevents oncogenic TGF-beta signaling and metastasis. Breast Cancer Res. 2009; 11:R68. [PubMed: 19740433]
42. Huanwen W, Zhiyong L, Xiaohua S, Xinyu R, Kai W, Tonghua L. Intrinsic chemoresistance to gemcitabine is associated with constitutive and laminin-induced phosphorylation of FAK in pancreatic cancer cell lines. Mol Cancer. 2009; 8:125. [PubMed: 20021699]
43. Ocak S, Yamashita H, Udyavar AR, Miller AN, Gonzalez AL, Zou YJ, et al. DNA copy number aberrations in small-cell lung cancer reveal activation of the focal adhesion pathway. Oncogene. 2010; 29:6331–42. [PubMed: 20802517]
44. Soffer SZ, Kim E, Moore JT, Huang J, Yokoi A, Manley C, et al. Novel use of an established agent: Topotecan is anti-angiogenic in experimental Wilms tumor. J Pediatr Surg. 2001; 36:1781–4. [PubMed: 11733906]
45. Lee A, Frischer J, Serur A, Huang J, Bae JO, Kornfield ZN, et al. Inhibition of cyclooxygenase-2 disrupts tumor vascular mural cell recruitment and survival signaling. Cancer Res. 2006; 66:4378–84. [PubMed: 16618763]
46. Golubovskaya VM, Ho B, Zheng M, Magis A, Ostrov D, Cance WG. Mitoxantrone targets the ATP-binding site of FAK, binds the FAK kinase domain and decreases FAK, Pyk-2, c-Src, and IGF-1R in vitro kinase activities. Anticancer Agents Med Chem. 2013; 13:546–54. [PubMed: 22292772]
47. Golubovskaya VM, Huang G, Ho B, Yemma M, Morrison CD, Lee J, et al. Pharmacologic blockade of FAK autophosphorylation decreases human glioblastoma tumor growth and synergizes with temozolomide. Mol Cancer Ther. 2013; 12:162–72. [PubMed: 23243059]

Implications

These data provide an initial understanding the tumorigenesis of difficult to treat renal tumors and provide an impetus for new avenues of research and potential for novel, targeted therapies.

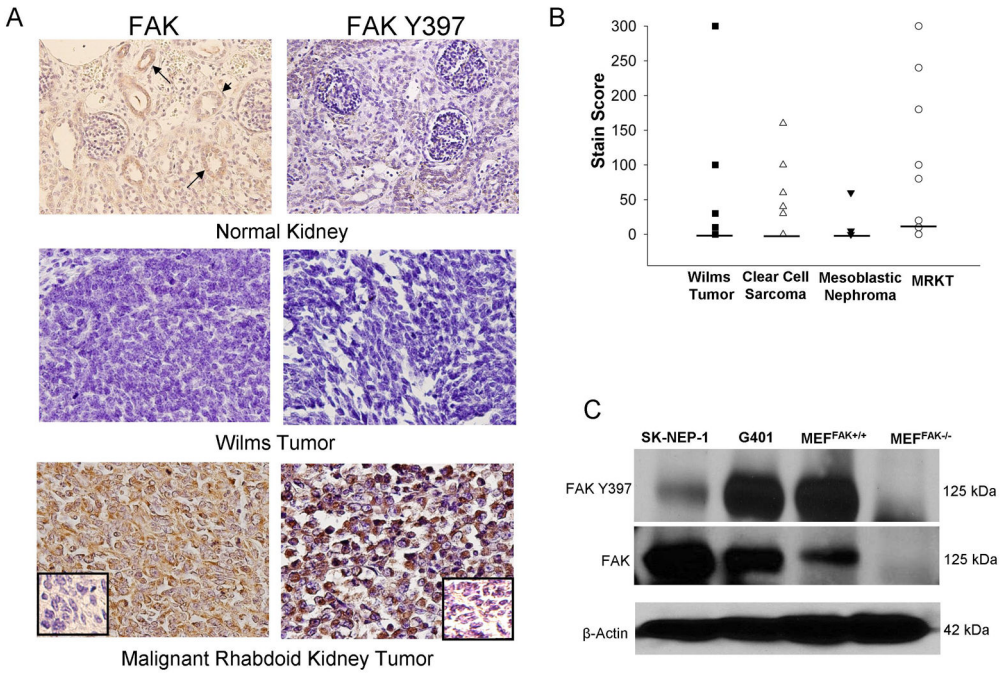

Figure 1.

FAK in pediatric renal tumor specimens and cell lines. **A.** Immunohistocemistry staining with antibodies specific for FAK and phospho-FAK was perfomed on 55 formalin-fixed, paraffin-embedded human pediatric renal tumor specimens (12 malignant rhabdoid kidney tumor, 12 clear cell sarcoma, 19 Wilms tumor, and 12 mesoblastic nephroma). Representative photomicrographs presented show weak FAK staining in the eipthelium of the renal tubules (*top left panel*, *closed arrows*) but no FAK phosphorylation (*top right panel*) in normal human kidney. Staining for FAK and phospho-FAK was not present in the majority of Wilms tumor specimens (*middle panels*). Strong staining for FAK and phospho-FAK was noted in most of the malignant rhabdoid kidney tumor specimens (*bottom panels*). Negative controls were included with each run (*inserts, bottom panels*). **B.** Stain scores were calculated for the IHC specimens listed above and reported as the range and median (*bar*). All tumor types, except for the MRKT, had a median stain score of 0. The median stain score for the MRKT specimens was 15. **C.** Immunoblotting for Y397 FAK and total FAK was performed on SK-NEP-1 and G401 renal tumor cell lysates. FAK was detected in both of the renal tumor cell lines and was phosphorylated. Lysates from mouse endothelial fibroblasts with ($MEF^{FAK+/+}$) and without ($MEF^{FAK-/-}$) FAK served as controls.

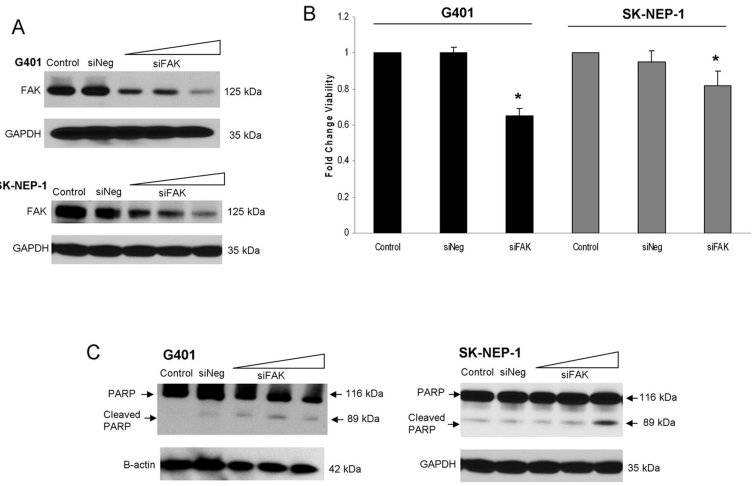

Figure 2.

FAK inhibition with siRNA in G401 and SK-NEP-1 human renal tumor cell lines. G401 and SK-NEP-1 cells were treated with HiPerFect® alone (control), negative control siRNA (siNeg), or siRNA specific for FAK (siFAK, 20, 40, 60 nM) for 24 hours. **A.** Immunoblotting for FAK showed decreased FAK expression in the G401 cells with 20 nM siFAK and in the SK-NEP-1 cells with 40 nM siFAK. Treatment with siNeg did not affect FAK expression. **B.** G401 and SK-NEP-1 cells were treated with siFAK for 24 hours (20 nM and 40 nM, respectively), cellular viability was measured using trypan blue exclusion, and reported as fold change in viability. In both cell lines, viability decreased significantly following treatment with siFAK. Cell viability was not affected by the siNeg treatment. Experiments were repeated at least in triplicate and data reported as mean fold change ± SEM. **C.** G401 and SK-NEP-1 cells were treated with increasing doses of siFAK for 24 hours and lysates examined with immunoblotting for PARP cleavage products. Increasing amounts of siFAK led to PARP cleavage, indicating apoptosis. siNeg did not result in PARP cleavage in either cell line.

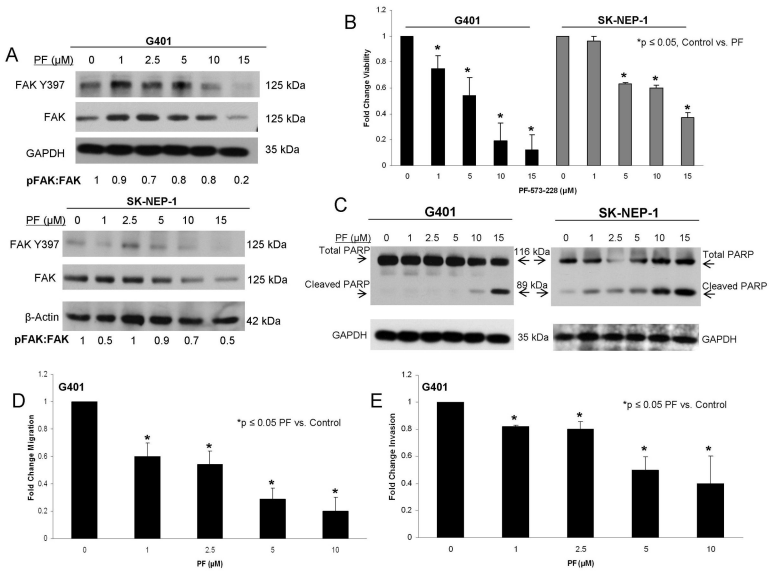

Figure 3.

PF-573,228 (PF) inhibition of FAK in human renal tumor cell lines. **A.** G401 and SK-NEP-1 cell lines were treated for 24 hours with increasing concentrations of PF-573,228 (PF). Cell lysates were harvested and evaluated with immunoblotting for total FAK and FAK Y397. Densitometry was performed, and FAK phosphorylation was reported as a ratio between the densities of the Y397 band to the total FAK band. Increasing concentrations of PF led to decreased FAK phosphorylation (Y397) in both cell lines. **B.** AlamarBlue® assays were used to assess cell survival. Both G401 and SK-NEP-1 cell lines showed significantly decreased cell survival following treatment with PF for 24 hours. **C.** Immunoblotting for cleaved PARP was utilized to detect apoptosis. G401 and SK-NEP-1 cells were treated with PF for 24 hours and cell lysates collected. Immunoblotting showed increased cleaved PARP following PF treatment in both cell lines, indicating apoptosis. **D.** G401 cells were treated with PF at increasing concentrations and allowed to migrate through a micropore insert. Migration was reported as fold change in the number of cells migrating through the membrane. Cellular migration was significantly diminished following treatment with PF. These effects were seen at a concentration of 1 μM PF. **E.** G401 cells were treated with increasing concentrations of PF and allowed to invade through a Matrigel™ coated micropore insert. Cells were counted and invasion reported as fold change. Invasion, similar to migration, was significantly decreased after exposure to 1 μM PF. All experiments were repeated at least in triplicate and data reported as mean fold change ± SEM.

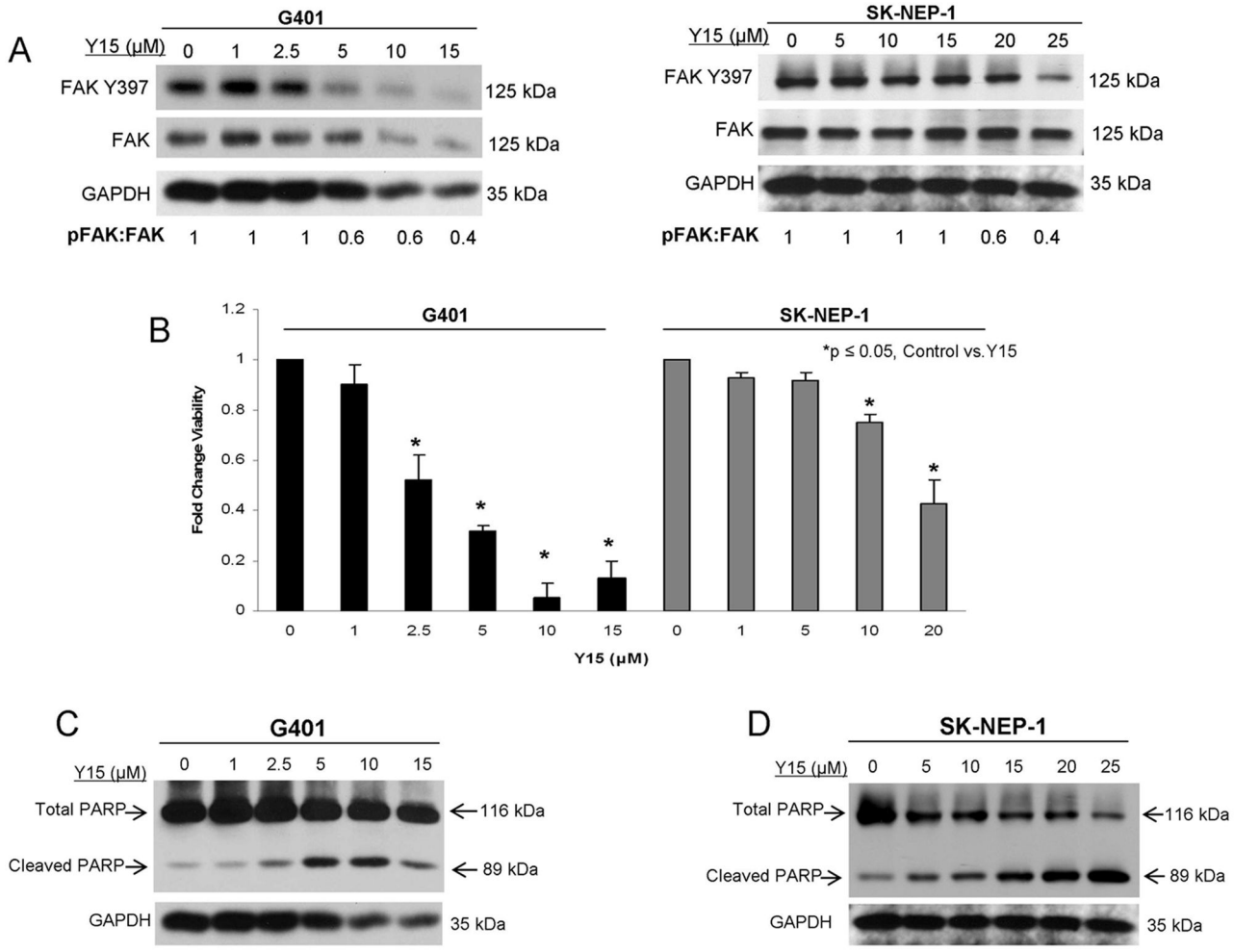

Figure 4.

1,2,4,5,-benzenetetraamine tetrahydrochloride (Y15) inhibition of FAK in human renal tumor cell lines. Investigations with another small molecule FAK inhibitor, Y15, were initiated in anticipation of advancing to *in vivo* experiments, knowing that PF-573,228 was not formulated for animals. **A.** G401 and SK-NEP-1 cells were treated with increasing concentrations of Y15 for 24 hours and lysates collected. Immunoblotting showed decreased FAK phosphorylation in both cell lines. Densitometry was performed, and FAK phosphorylation was reported as a ratio between the density of the Y397 band to the total FAK band, confirming decreased FAK phosphorylation. **B.** AlamarBlue® assay was used to measure cell viability. G401 and SK-NEP-1 cells were treated with Y15 at increasing concentrations for 24 hours. Cellular viability was decreased with treatment of 2.5 μM concentration in the G401 and 10 μM concentration in the SK-NEP-1 cell line. Experiments were repeated at least in triplicate and data reported as mean fold change ± SEM. **C.** Immunoblotting was utilized to detect apoptosis. There was a decrease in total PARP and an increase in cleaved PARP detected in cell lysates from the G401 cell line after Y15. **D.** Immunoblotting was utilized to detect apoptosis in the SK-NEP-1 cell line following Y15

treatment. Y15 induced apoptosis as demonstrated by a decrease in total PARP and an increase in cleaved PARP.

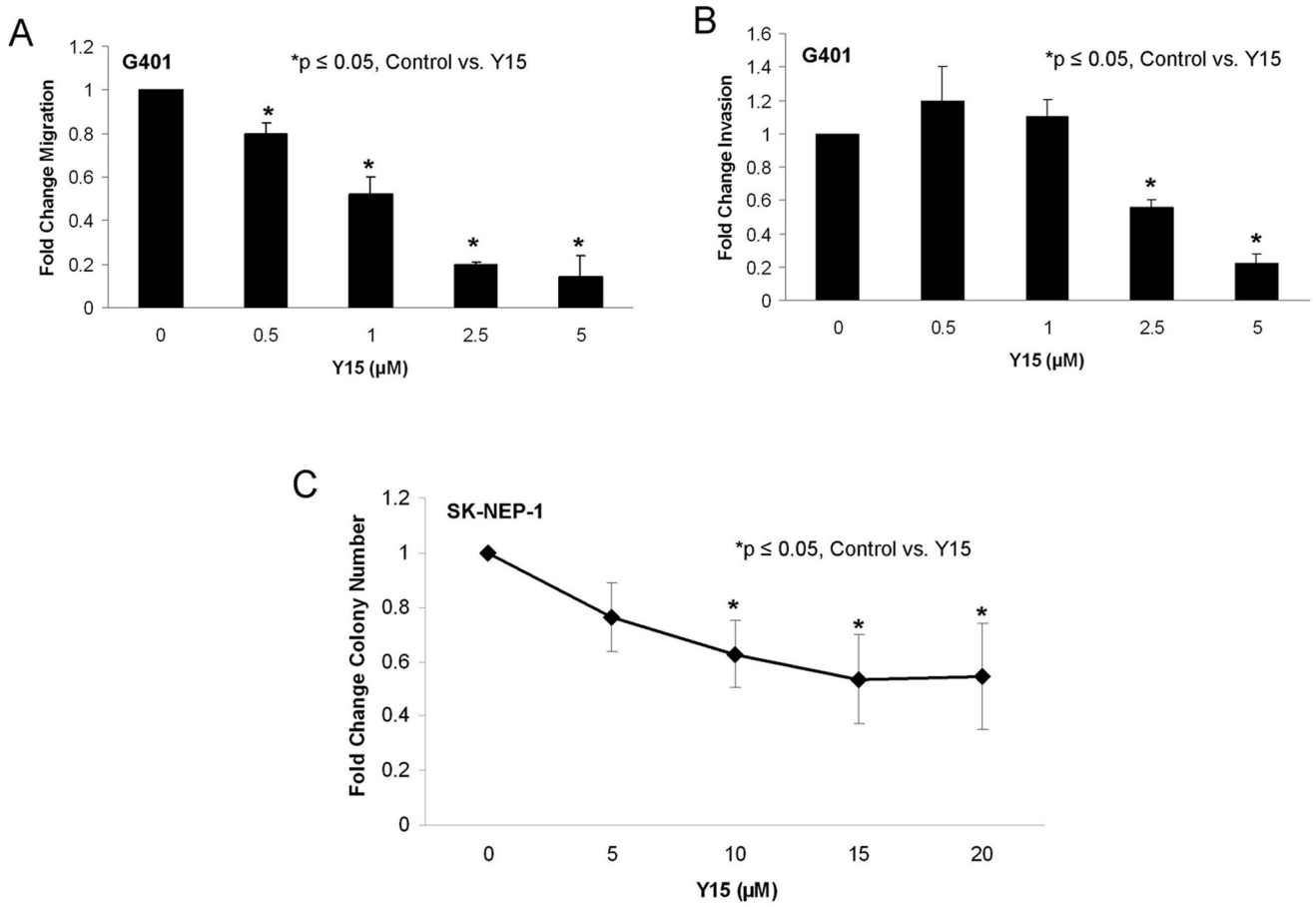

Figure 5.

1,2,3,4-benzenetetraamine tetrahydrochloride (Y15) decreased cell migration, invasion, and attachment independent growth. **A.** G401 cells were treated with increasing concentrations of Y15 for 24 hours and allowed to migrate through a micropore insert. Migration was reported as fold change in number of cells migrating through the membrane. Cellular migration was significantly decreased with Y15 treatment, beginning at 0.5 μM concentration. **B.** G401 cells were treated with increasing concentrations of Y15 and allowed to invade through a Matrigel™ coated micropore insert. Invasion was reported as fold change. Cellular invasion was significantly decreased with increasing concentrations of Y15. **C.** Attachment independent growth in soft agar was utilized to characterize tumor invasiveness in the SK-NEP-1 cells. Cells were treated with increasing concentrations of Y15, grown in soft agar for 6 weeks, and colonies were quantified. Colony count was significantly decreased with Y15 treatment compared to untreated cells. All experiments were repeated at least in triplicate and data reported as mean fold change ± SEM.

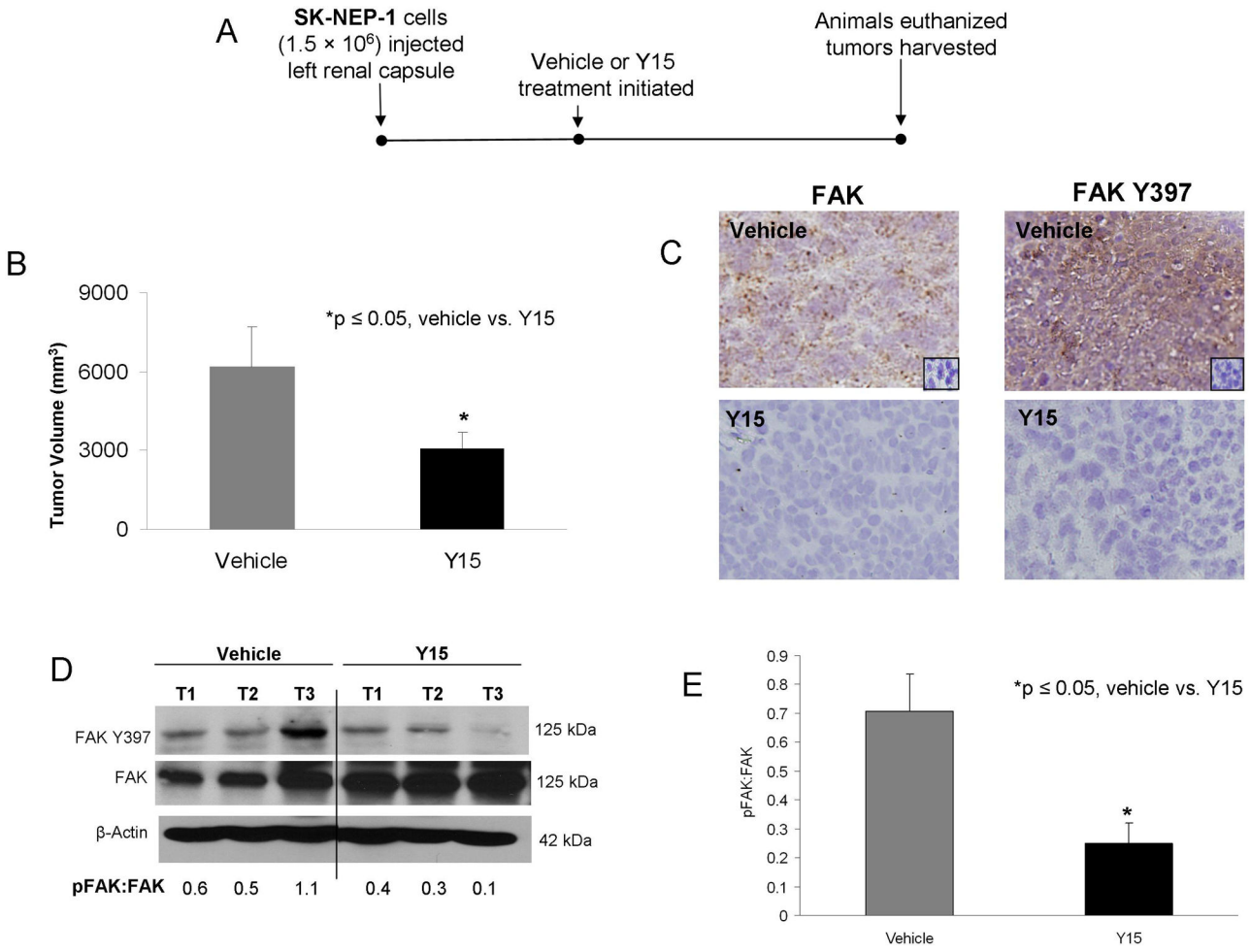

Figure 6.

Treatment with 1,2,4,5-benzenetetraamine tetrahydrochloride (Y15) inhibited growth of human renal tumor xenografts. The investigations were advanced to a nude mouse xenograft model. **A.** Experimental time line. SK-NEP-1 cells were injected into the subcapsular space of the left kidney. After two weeks, animals were randomized to receive twice daily intraperitoneal injections of vehicle (n = 7, sterile normal saline, control, 100 μL) or Y15 (n = 8, 30 mg/kg/day, 100 μL). Animals were euthanized after 21 days treatment and their tumors harvested for study. **B.** Tumor volumes were measured when animals euthanized. Animals treated with Y15 had significantly smaller tumors than animals treated with control vehicle. **C.** Representative photomicrographs at 40 × of immunohistochemical staining of the formalin fixed, paraffin-embedded SK-NEP-1 xenograft samples. Immunohistochemical staining showed that the tumors from animals treated with Y15 had decreased FAK Y397 phosphorylation (*bottom right panel*) compared to vehicle treated tumors (*top right panel*). Negative controls (mouse or rabbit IgG) were performed with each run (*inserts top panels*). **D.** To further confirm target knockdown in the tumor specimens, immunoblotting for FAK Y397 was performed on xenograft tumor lysates. Tumors were homogenized and proteins separated on SDS-PAGE gels, immunoblotting for Y397 and total FAK were performed, with a representative immunoblot shown. There was a decrease in FAK phosphorylation

(Y397) in the tumors from the animals that received Y15 treatment. These findings were further demonstrated by densitometry, reported as pFAK:FAK ratio. **E.** Immunoblots from a number of xenograft specimens were analyzed with densitometry. Phosphorylated FAK was expressed as a ratio to total FAK for each blot and normalized to the β-actin for that blot, allowing for a comparison to be made between the saline treated and the Y15 treated tumors. There was a significant decrease in the FAK phosphorylation (Y397) in the tumors from the animals treated with Y15.

Table 1

Immunohistochemical staining for phosphorylated and total FAK in pediatric renal tumor specimens.

Tumor Type	n	FAK 4.47 (%)	pFAK Y397 (%)	P Value (vs. MRKT)
Malignant Rhabdoid Kidney Tumor	12	9 (75)	6 (50)	-
Clear Cell Sarcoma	12	4 (33)	1 (8)	NS
Wilms Tumor	19	6 (32)	4 (21)	0.03
Mesoblastic Nephroma	12	1 (8)	0 (0)	0.003

FAK 4.47 = total FAK protein; **pFAK Y397** = FAK phosphorylated at tyrosine 397 residue